Published online July 18, 2005

Water and Solute Transport in a Cultivated Silt Loam Soil: 1. Field Observations

Y. Coquet,* C. Coutadeur, C. Labat, P. Vachier, M. Th. van Genuchten, J. Roger-Estrade, and J. Šimůnek

ABSTRACT

Vadose zone flow and transport processes are known to be strongly affected by both soil structure and soil texture. We conducted a field experiment to explore the impact of heterogeneity in soil structure created by agricultural operations such as wheel traffic, plowing, and surface tillage on water and solute transport. The experiment was performed on a 4 by 2 m^2 field plot perpendicular to the path of a tractor that had pulled a harrow for seedbed preparation. The plot was irrigated with a rainfall simulator at a rate of 21 mm h^{-1} for 2 h and 20 min. An 850 mg L^{-1} bromide solution was subsequently applied at a rate of 26 mm h^{-1} for 2 h. Soil water contents and pressure heads during the experiment were monitored with time domain reflectometry (TDR) probes and tensiometers. The soil was sampled for resident bromide (Br^-) concentrations at the end of the experiment. Water and bromide fronts were found to be highly heterogeneous. The heterogeneity could be explained by the particular soil structural features created by the agricultural practices, in particular by the locations and sizes of compacted soil zones. Very little water and bromide had penetrated the large compacted zones under the wheel tracks. Bromide, TDR, and tensiometer measurements all indicated the presence of preferential flow of water and bromide along paths immediately bordering the wheel tracks. The compacted clods in the plow layer furthermore acted as low-permeability barriers that diverted water and bromide flow around them. The highly heterogeneous plow layer between the wheel tracks produced a much higher solute dispersivity as compared to the compacted soil below the wheel tracks.

Numerous studies have shown that water and solute transport in soils can be highly heterogeneous at the field scale (e.g., Butters et al., 1989; Roth et al., 1991; Flury et al., 1994, 1995; Hammel et al., 1999). This fact makes it difficult to define and estimate equivalent or effective parameters for use in relatively simple models describing field behavior (Ellsworth and Jury, 1991; Mayer et al., 1999). Recently, Vanderborght et al. (1997, 2001) highlighted the importance of soil morphology in explaining prevailing solute transport properties. The presence of different horizons or layers within a soil can be a major factor causing flow heterogeneity (van Wesenbeck and Kachanoski, 1994; Deurer et al., 2001). In addition to the intrinsic structural properties associated with soil type, vadose zone flow and transport processes are also affected by such external factors as tillage practices. For example, Petersen et al. (1999, 2001) showed that surface tillage may strongly affect the dynamics of dye tracers in soils. Trafficking by agricultural or other machinery has also been shown to modify the hydraulic properties and porosity of soils (Meek et al., 1989; Ankeny et al., 1990; Mohanty et al., 1994; Gysi et al., 1999). A major challenge is to find useful proxy variables to assess soil structure heterogeneity (Young et al., 2001).

The structure of tilled soils is known to be strongly affected by agricultural practices to which the field is subjected. For instance, heavy compaction by the wheels of farm machinery will produce an abundance of compacted clods within the tilled layer once the soil is plowed (Roger-Estrade et al., 2000), especially for relatively fine-textured soils. On the other hand, surface tillage may lead to the destruction of compacted clods that were initially present in the plow layer. This disintegration of clods is generally limited to the surface few centimeters of the plow layer (i.e., the seed bed).

To better describe the effects of agricultural machinery on soil structure and compaction, Manichon (1982) proposed a field method for characterizing soil structure. The method pays particular attention to visible porosity and the compaction status of the soil. The tilled soil for this purpose was divided vertically into several layers or compartments consistent with the depth of various tillage operations. For instance, for cropping systems that include plowing, the vertical compartments immediately after sowing may include a seed bed, a plow layer that is unaffected by seed bed preparation, and the underlying undisturbed soil. Compartments were similarly separated laterally according to the locations of wheel tracks of tractors and other farm machinery that may have compacted the underlying soil. These compacted zones would alternate within the plow layer with noncompacted zones located between the wheel tracks. Manichon (1982) identified three different types of soil structure (Δ,Φ, and Γ), each having unique internal macroscopic porosities. These types of soil structure may hold for entire compartments if they are homogeneous (e.g., the relatively large compacted zone in the plow layer below the wheel tracks), or for particular clods within a more heterogeneous compartment (e.g., the plow layer between wheel tracks containing compacted clods originating from former wheel tracks, as well as noncompacted macroporous clods). Several studies have shown that these different compartments or clods can have significantly different saturated and unsaturated hydraulic properties (Curmi, 1987; Coutadeur et al., 2002).

Y. Coquet, C. Coutadeur, C. Labat, and P. Vachier, UMR INRA/INAPG Environment and Arable Crops, Institut National de la Recherche Agronomique/Institut National Agronomique Paris-Grignon, B.P. 01, 78850 Thiverval-Grignon, France; J. Roger-Estrade, UMR INRA/INAPG Agronomy, Institut National de la Recherche Agronomique/Institut National Agronomique Paris-Grignon, B.P. 01, 78850 Thiverval-Grignon, France; M.Th. van Genuchten, USDA-ARS, George E. Brown, Jr. Salinity Lab., 450 West Big Springs Road, Riverside, CA 92507; J. Šimůnek, Dep. of Environmental Sciences, Univ. of California, Riverside, CA 92521. Received 7 Oct. 2004. *Corresponding author (coquet@grignon.inra.fr).

Published in Vadose Zone Journal 4:573–586 (2005).
Original Research Paper
doi:10.2136/vzj2004.0152

677 S. Segoe Rd., Madison, WI 53711 USA

Abbreviations: HPLC, high performance liquid chromatography; TDR, time domain reflectometry.

The purpose of this study was to understand how the presence of different layers, compartments, or clods, resulting from tillage and trafficking, affect water and solute transport in an agricultural soil profile. Our hypothesis was that the simultaneous presence of compacted and more macroporous clods and aggregates will lead to considerable heterogeneity in the prevailing flow and transport processes. We tested this hypothesis on a silt loam soil whose cultivation was representative of cropping systems that include moldboard plowing. Our study involved a detailed field experiment to be discussed in this paper, as well as the use of a numerical model for optimal analysis of the data as described in Part 2 of this two-part series (Coquet et al., 2005).

MATERIALS AND METHODS

Site Characteristics and Tillage Practices

The experiment was conducted in an agricultural field of the Institut National de la Recherche Agronomique (INRA) Experimental Station at Grignon (Yvelines, France). The field was cropped each year since 1962 with maize (*Zea mays* L.). The soil is a silt loam Calcic Cambisol (FAO classification) overlaying dense limestone at a depth of 90 cm. The plow layer (0–30 cm) consisted on average of 28.2% clay (<2 μm), 61.2% silt (2–50 μm) and 6.5% sand (0.05–2 mm), and contained 2.2% organic matter and 1.3% calcium carbonate. The particle size distribution was determined using sedimentation and wet sieving methods after organic matter removal by H_2O_2 and decarbonation by HCl (Association Française de Normalisation [AFNOR], 1983), whereas the organic matter content was measured using dry combustion (AFNOR, 1995a), and the calcium carbonate content using a volumetric method (AFNOR, 1995b).

Consistent with local cultivation practices, the soil was plowed on 29 Nov. 2000, using a three-furrow moldboard plow. A seedbed (12–14 cm deep) was prepared on 7 May 2001 by means of two runs using a 3.0-m wide rotary harrow following the same tracks. The tractor had 40-cm wide rear tires, which were connected to 24-cm wide dual tires, with a space of 16 cm between the main and dual tires. The inner spacing between the two rear tires was 132 cm. The soil during the entire experiment was kept free from vegetation by manual weeding.

Structure of the Tilled Soil

The structure of the tilled soil was observed along the face of a large trench perpendicular to the tillage direction. The trench was 70 cm deep and 3.1 m wide to cover one complete unit of the spatially periodic soil structural pattern created by the tillage operation (i.e., seed bed preparation). The structure of the tilled soil was described using the scheme of Manichon (1982), which divides the profile into vertical and horizontal compartments according to the effects of tillage (i.e., soil fragmentation by tillage tools and compaction by wheels) together with a description of the internal structure of each compartment (Fig. 1). Manichon (1982) defined three types of internal structure (Δ,Φ, and Γ) as explained below:

- **Δ structure with No Structural Porosity and Smoothly Breaking Faces.** This type of soil structure is created by compaction under the wheel tracks of tractors or other heavy farm machinery. The Δ structure is also characteristic of clods located in the plow layer between the wheels tracks. Such Δ clods are created by plowing that cuts and fragments the compacted soil formed under former wheel tracks.
- **Φ Structure Stemming from Δ-Structured Soil, but Containing Incipient Cracks Due to Swelling/Shrinkage Processes and Freezing/Thawing Cycles.** This type of soil structure appears in the upper part of the tilled soil where the effects of climate are the most significant (i.e., the upper part of the compacted zones below the wheel tracks, and compacted clods in the upper part of the plow layer).
- **Γ Structure Formed by the Coalescence of Macroporous Aggregates or Clods, with Structural Porosity Clearly Visible to the Eye.**

The above three types of structure, as well as regular uncompacted soil (defined here as clods or aggregates <2 cm), are present in the plow layer of most cultivated soils. The relative proportion, size, and location of each of the three structure types are generally specific of the adopted cropping system (Richard et al., 1999; Roger-Estrade et al., 2000).

The structure of the soil profile was described three times during the experiment according to above criteria. The first time was immediately before installation of the TDR probes and tensiometers used to monitor soil water status during the experiment. The probes were inserted in the soil to a distance of 30 cm from the face of the trench and distributed over the profile in such a way that most or all compartments and clod types would be sampled by at least one TDR probe and one tensiometer, based on the structure that could be seen along the face of the installation trench. Soil structure type was also determined at the time when gravimetric soil samples were taken for concentration measurements of Br^- added at the start of the experiment. The local structure of the soil in terms of Δ, Φ, or Γ status was determined just before collecting the soil samples. Finally, the structure was described a third time when the TDR probes and tensiometers were removed, thus yielding accurate information about the actual Δ, Φ, or Γ structure around each probe.

Experimental Set-up

The experiment started with a rainfall simulation on 6 June 2001, using a large rainfall simulator composed of a Tee Jet 80010 nozzle placed on a swinging arm positioned 3.7 m above the soil surface. A plot of 4 by 2 m^2 was uniformly irrigated by protecting the spray from wind or local turbulence using a large framed tent. The plot had its longer dimension perpendicular to the moving direction of the farm machinery, and was centered along the axis of the path of the tractor pulling the harrow for seed bed preparation. The uniformity of water application within the plot had been previously measured several times using 24 tin cans evenly distributed over the irrigated surface. The simulated rainfall had coefficients of variation (CV) ranging from 17 to 30% depending on the feeding pressure of the nozzle. Tap water was used for 260 min at a rainfall intensity of 21 mm h^{-1}. Electrical conductivity of the tap water was 745 μS cm^{-1}; pH was 7.9; total and temporary hardness were 250 and 350 mmol L^{-1}, respectively; and chloride, nitrate and sulfate concentrations were 39, 30, and 64 mg L^{-1}, respectively. The Br^- concentration of the tap water was <0.1 mg L^{-1}.

The initial rainfall simulation was followed by application of a KBr solution at 850 mg L^{-1} Br^- for 2 h at a rainfall intensity of 26 mm h^{-1}. The CV of the Br^- application was 21% and that of the water application before Br^- was 25%. After Br^- application, the irrigated surface was covered with thick impermeable plastic to shield the soil from any natural rain during water redistribution within the soil between 6 June and 17 July. No temporal change in soil structure due to

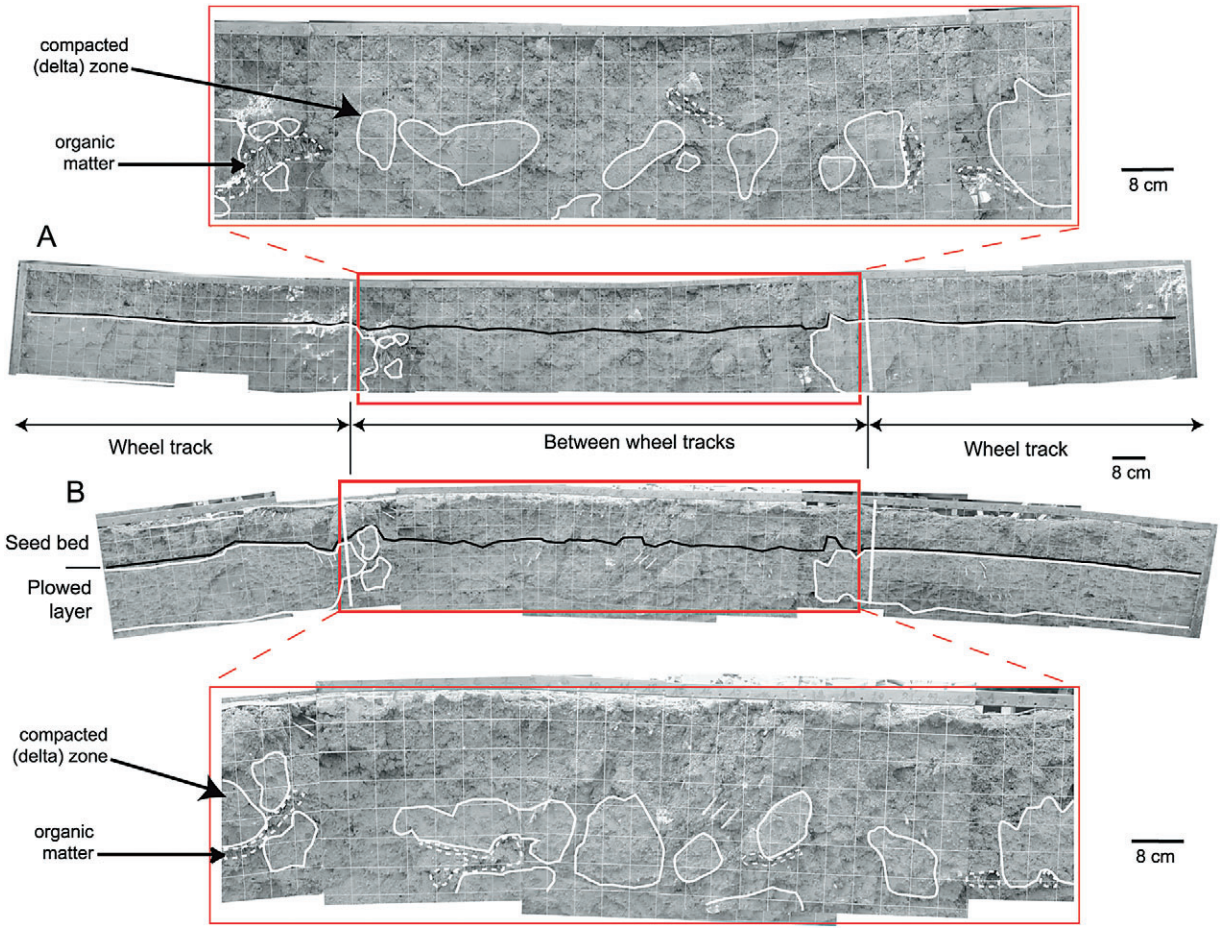

Fig. 1. Soil profiles showing the partitioning of the tilled layer. Compacted Δ soil is delineated by solid white lines. Boundaries between the seedbed and the plow layer are indicated by a solid black line. Accumulations of organic matter residues are surrounded by dotted white lines. (A) Soil profile that was sampled for bromide. (B) Soil profile where time domain reflectometry (TDR) probes and tensiometers were installed. Note that the bending of the pictures is due to uncorrected parallax effects and not to actual topography.

swelling/shrinkage or dispersion/deposition of clay particles could be detected during the entire experiment. This was due to the fact that the clay fraction of the soil contained a limited amount of swelling clay minerals. No anion exclusion was expected in the soil as previous experiments with the same soil showed that bromide transport was similar to the transport of water isotopic tracers. Additional details about the experimental setup are given by Desbourdes-Coutadeur (2002).

Soil Water Content and Pressure Head Measurements

Thirty 20-cm-long TDR probes and 30 mini-tensiometers were installed in the soil profile (Fig. 2a). The mini-tensiometers had 2-cm-long, 6-mm-diam. ceramic ends mounted on 80-cm-long soft translucent PVC tubes connected to mercury manometers.

To accommodate installation of the probes, a trench (70 cm deep and 3.1 m wide) was excavated such that its main face was perpendicular to the moving direction of the farm machinery. Probes were installed through horizontal holes dug into one of the main faces (Fig. 3). The lengths of the holes (20 cm for the TDR probes, 29 cm for the tensiometers) were taken such that the middle parts of the probes (10 cm for the TDR probes, 1 cm for the tensiometers) would be situated at positions 30 cm from the main face of the trench. TDR probes were inserted directly by pushing them through the end of the holes, whereas holes slightly larger than the ceramic cups were used for the tensiometers. To improve contact with the soil, the tensiometer cups were dipped in a soil slurry before inserting them. The TDR cables and flexible tensiometer tubes were routed laterally through the holes that were repacked with soil previously excavated from those locations, and then up to the soil surface through the refilled trench. Thus, the probes were placed 30 cm into the undisturbed soil below the irrigated plot (Fig. 3). This setup kept the soil below the irrigated plot as undisturbed as possible. Also, the refilled installation trench did not directly receive irrigation water, thus preventing any water from infiltrating preferentially along the cables or tubes toward the probes.

All TDR probes were connected to a single acquisition system (TRASE, Soil Moisture Equipment Corp., Santa Barbara, CA) to obtain volumetric water content (θ) data for each probe every 11 min (the minimum time required to scan all 30 probes), while the mercury manometers of the tensiometers were read manually. The TDR and tensiometer measurements were recorded essentially continuously for 380 min during the infiltration part of the experiment. The measurements during redistribution were performed at increasingly larger time intervals from 4 h to 14 d (6 June–17 July 2001).

Solute Concentration Measurements

A map of Br^- resident concentrations was constructed by sampling the soil destructively 12 h after the rainfall simulation. Soil was collected through a new access trench excavated in the 4 by 2 m plot that was previously irrigated with water

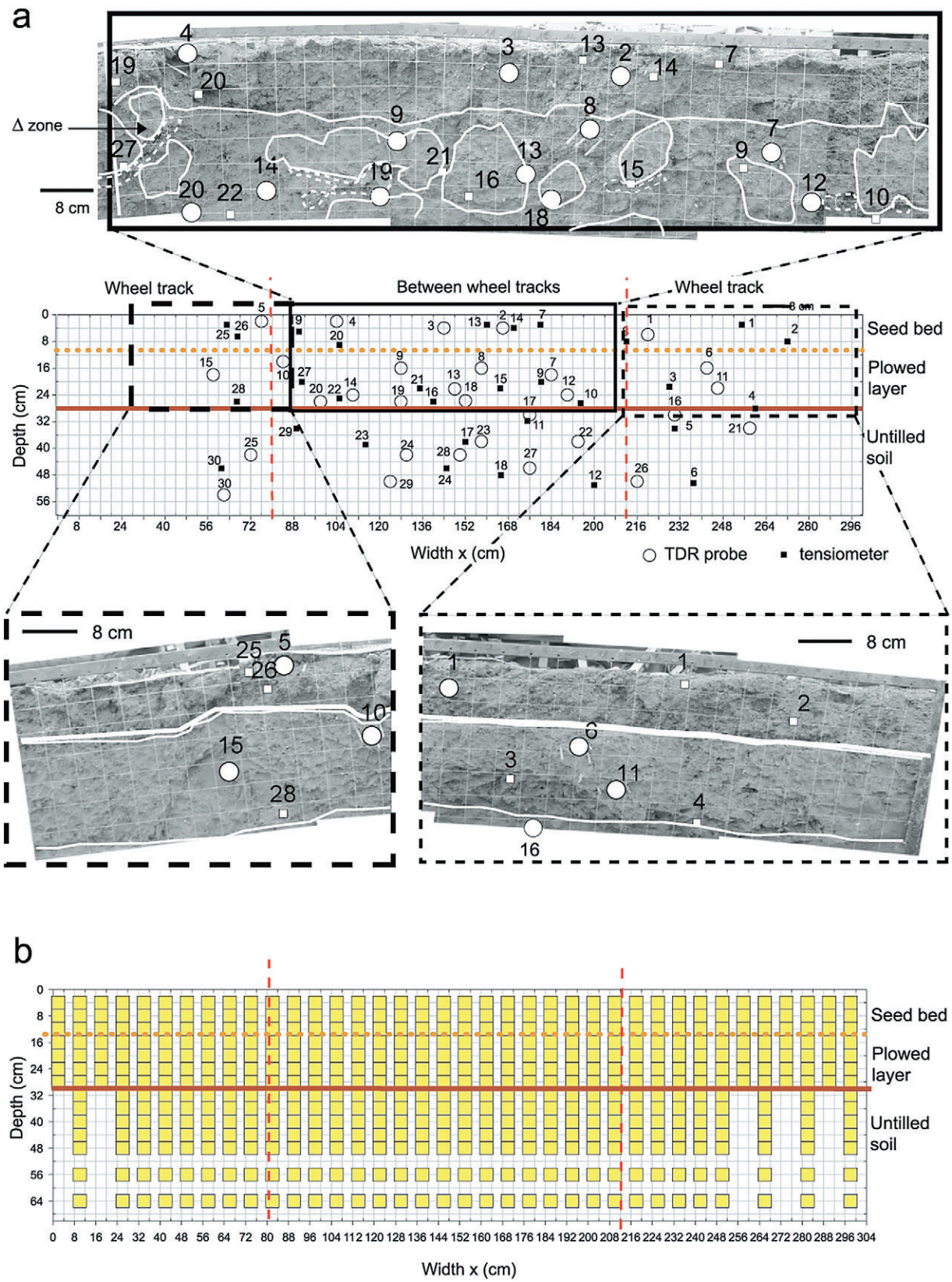

Fig. 2. (a) Locations of time domain reflectometry (TDR) probes (large circles) and tensiometers (small squares) within the soil profile. The enlarged pictures show the position of the TDR probes and tensiometers in relation to the structure of the plow layer. Solid white lines delineate compacted Δ soil as well as the boundary between the seedbed and the plow layer. Accumulations of organic matter residues are delineated by dotted white lines. (b) Locations of the samples taken from the soil for bromide measurements.

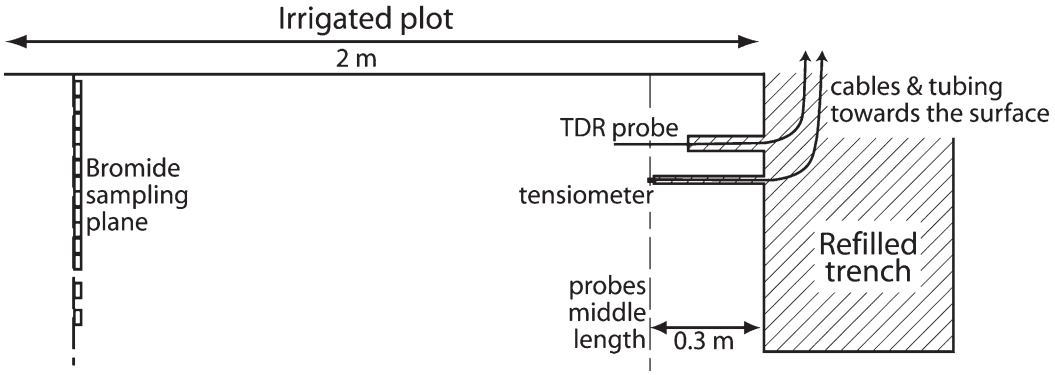

Fig. 3. Vertical cross-section showing the installation of the time domain reflectometry (TDR) probes and tensiometers. The cross-section is perpendicular to the main direction of the installation trench and parallel to the moving direction of the farm machinery.

and Br^- (Fig. 3). The trench had the same orientation as the trench used for installing the TDR probes and tensiometers. The main face oriented toward the center of the irrigated plot (i.e., toward the instrumented face of the probe-installation trench; Fig. 3) was intensively sampled using small cylinders (4-cm diam., 2-cm height) every 8 cm in the horizontal direction along a distance of 300 cm, and every 4 cm in the vertical direction starting at a depth of 4 cm down to 48 cm, and also at the 56- and 64-cm depths (Fig. 2b). A few vertical sampling profiles were not completed below the dual tire tracks where little Br^- transport was expected. A total of 597 small cores were taken from precisely measured locations using a framed square grid. The trench was not refilled, but its face was covered with plastic. The Br^--sampling trench was thought to be far enough (1.2 m) from the TDR probes and tensiometers to limit its impact on the flow and transport measurements.

After sampling, the cores were brought immediately to the laboratory, weighed, placed in an oven (105°C) for 48 h and then reweighed to obtain their volumetric and gravimetric water contents. The complete dry samples were subsequently transferred into 500-mL plastic centrifugation tubes and weighed again. After adding about 40 mL of deionized water to the dry samples (i.e., between once and twice their dry weight), the tubes were agitated for 20 h and centrifuged for 20 min at 8000 rpm. The supernatant was filtered through a 1.2-μm glass microfiber filter (Whatman GF/C cat 1822 090, Whatman International Ltd, Maidstone, UK) and stored <30 d in a 30-mL plastic flask at 4°C in a cold chamber before analysis for Br^-.

Bromide concentrations of the extracted liquid were measured using a high performance liquid chromatography (HPLC) chain composed of an automatic sampler (Waters 717 autosampler, Waters Corp., Milford, MA), a pump and a gradient controller (Waters 600E controller system), and a diode array detector (Waters 996). The HPLC column was of the anion-exchange type (Waters IC Pack HC) composed of a polymethylacrylate resin grafted with quaternary ammoniums, and preceded by a pre-column of the same type. A 1-mL aliquot of the extracted liquid phase was filtered again on a 0.45-μm nylon filter (no. FS13N45, A.I.T., Le Mesnil le Roi, France) and placed in the automatic sampler. A volume of 100 μL was injected into the column with a mobile phase of potassium dihydrogen phosphate at 30 mmol L^{-1} containing 20% acetonitrile. The mobile phase was adjusted to pH of 2.8 with phosphoric acid. The mobile phase was also filtered through a 0.45-μm membrane filter (Durapor cat. HVLPO4700, Millipore Corp., Billerica, MA) before entering the column at a rate of 2 mL min^{-1}. The wavelength of detection was set at 205 nm, while the retention time of Br^- under the prevailing conditions was 21 min. The chromatography assay lasted about 30 min to allow for the removal of nitrates and chlorides from the column before a new injection.

RESULTS AND DISCUSSION

Structure of the Tilled Soil

Three layers could be identified in the soil profile (Fig. 1): a seed bed (0–12 cm) which had been created by harrowing the plow layer, a plow layer (12–30 cm) unaffected by surface tillage, and soil below the plow layer (>30 cm; not shown in Fig. 1) which had not been disturbed by tillage. No plow pan could be identified since the plowing depth had been increased to 30 cm by the farmer the year the experiment took place, instead of 28 cm in previous years. The second layer (the plow layer that had not been harrowed) could be further divided laterally into compacted zones affected by the wheels of the tractor pulling the harrow, and zones between the wheel tracks that were not affected by compaction.

The seed bed consisted of mostly very loose soil with only a few small Δ and Φ clods (<10 cm) that were left unfragmented by the harrow. The plow layer below the wheel tracks appeared in the form of large homogeneous Δ zones. These compacted zones extended slightly in lateral directions from the wheel tracks (Fig. 1) because of mechanical stress exerted by the wheels. The plow layer between the wheel tracks was the most heterogeneous, containing both Γ and Δ clods. The Δ clods originated from old compacted zones below former wheel tracks (e.g., during harvesting of the preceding maize crop) but displaced and fragmented by the last plowing. Φ clods were almost absent during the year of the experiment, which was consistent with the fact that the freezing depth during the relatively mild winter of 2000/2001 was only about 10 cm. Finally, the untilled soil appeared very homogeneous at the macroscopic scale; the only visible structural features were earthworm (*Lumbricus terrestris*) holes and decayed plant root channels.

To evaluate soil structural variability in the longitudinal direction (i.e., in the direction the tractor moved), we compared the different profile descriptions made along the same tractor path. The compacted Δ zones below the wheel tracks (surrounded by white lines in

Fig. 1) are clearly visible in the two profiles, and intruded into the area between the wheel tracks. The plow layer between the wheel tracks is shown enlarged in Fig. 1. The continuous white lines in the enlarged pictures again delineate compacted zones, whereas the discontinuous white lines highlight organic matter residues. Notice that the compacted zones on the sides below the wheel tracks have similar shapes and extents in both profiles. In particular, the compacted zone on the left side shows the same inclusion of organic matter derived from maize stems and root residues located along the same row and buried by plowing. Also notice the large Δ clods (split into two pieces in Profile A) 12 cm to the right of the left wheel track (the grid mesh is 4 cm in the pictures) in both profiles. These large clods resulted from a compacted Δ band under a former wheel track, which was cut and displaced by the last plowing. Other Δ clods of smaller sizes are visible in both profiles, with quite similar locations within the profiles.

The similarities between the soil profiles within the same tractor passage suggest that longitudinal variability in soil structure created by tillage is much smaller than lateral variability. This finding motivated us to experimentally and numerically study the transport problem in terms of a two-dimensional vertical analysis (i.e., along a cross-sectional area perpendicular to the path of the tillage machinery).

Soil Water Dynamics in the Tilled Soil

Observed Water Contents During Infiltration

Volumetric water contents (θ) vs. time were measured at 29 of 30 TDR locations within the tilled soil (one TDR probe, No. 6, was found to be unreliable because of bending of the rods during installation). Time zero was at the start of the rainfall simulation. The initial water content of the seed bed (Fig. 4a) was homogeneous and very low (close to 0.05 $m^3\ m^{-3}$). Similar low values in the very top of seed beds were previously measured by Sillon (1999) for a comparable soil during evaporation. The five TDR probes in the upper part of the seed bed between 2 and 6 cm depth all indicated similar water contents vs. time, with a rapid increase in θ shortly after starting the rainfall simulation. The water contents then reached a plateau at values (~0.20–0.30 $m^3\ m^{-3}$) which were very similar for Probes 2, 3, 4, and 5, and slightly higher for Probe 1. These values are much lower than the saturated water content of the seed bed which had been estimated to be 0.54 $m^3\ m^{-3}$ based on slow resaturation of large soil cylinders (15-cm diam., 7-cm height) in the laboratory. The plateau values increased slightly after 4.5 h when the rainfall intensity was increased from 21 to 26 mm h^{-1} during Br^- application.

Water contents of the plow layer are plotted separately in Fig. 4b for probes in the compacted Δ zones, and in Fig. 4c for probes in the macroporous Γ zones. The initial water content was generally higher and less variable in Δ zones than in Γ structures. Probes located within the Δ zones were further separated into two groups. The first group, which included Probes 11, 15, and 18, had high initial water contents (about 0.38 $m^3\ m^{-3}$) and showed little or no response to the infiltration. The second group, consisting of Probes 9, 19, and 20, showed a noticeable increase in water content following infiltration. The response of each of the TDR probes of this second group can be explained by considering their particular location within the tilled soil (Fig. 2). For example, Probe 9 was located within a Δ zone, but at the very top of a large clod immediately below the seed bed. Also, a small crack was visible in the top part of this Δ clod directly above the right waveguide of the probe. That probe had its measurement volume partly in a Γ zone and partly in a Δ clod, thus recording water contents that were intermediate between the Γ zones (i.e., the probes of Fig. 4c) and Δ zones (i.e., Probes 11, 15, and 18 in Fig. 4b). Probe 20 next to the left wheel track was actually in a Γ zone, while Probe 19 was located immediately below a high organic matter area with high porosity as judged from visual examination.

The TDR probes in the Γ zones showed substantial increases in water content after 1 h of infiltration (Fig. 4c). Similarly, as for the seed bed, plateau values slightly increased when the rainfall intensity was changed. The plateau values of the water content of the Γ zones were close to the saturated water content of the Γ soil (estimated to be 0.39 $m^3 m^{-3}$ from laboratory measurements on large cylinders as done for the seedbed). The initial water content measured with each probe reflected the depth of that probe. For instance, Probes 12 and 14 were located at 24 cm depth and Probe 8 at 16 cm depth.

For the deeper soil layer that remained undisturbed by tillage, we separated between probes located below the wheel tracks (Fig. 4d) and those between the wheel tracks (Fig. 4e). The initial water content was more heterogeneous between the wheel tracks than below. This was most likely due to heterogeneity in water fluxes within the plow layer between the wheel tracks before the experiment. The water content of probes between the wheel tracks increased more rapidly than those below the wheel tracks, except for Probe 26, which was located very close to the right wheel track (Fig. 2a). Assuming that little or no water infiltrated through the compacted Δ zones below the wheel tracks, the slow increase in water content as shown by the TDR probes in the untilled soil below the wheel tracks (Fig. 4d, Probes 25, 30) must have been due to some lateral flow of water that infiltrated between the wheel tracks.

Observed Pressure Heads During Infiltration

Initial pressure heads in the seed bed (Fig. 5a) varied between −100 and −600 cm without much correlation with depth. Tensiometers 1, 7, 13, and 25 were all located at a depth of 3 cm, but had initial pressure heads of −180, −420, −100, and −520 cm, respectively. We attribute these relatively large differences to local variations in the redistribution of water that either was added initially around the tensiometer cups during installation, or had leaked from the cups during flushing of the tensiometers to remove air bubbles before the experiment. Similar to the TDR probes, the tensiometers recorded

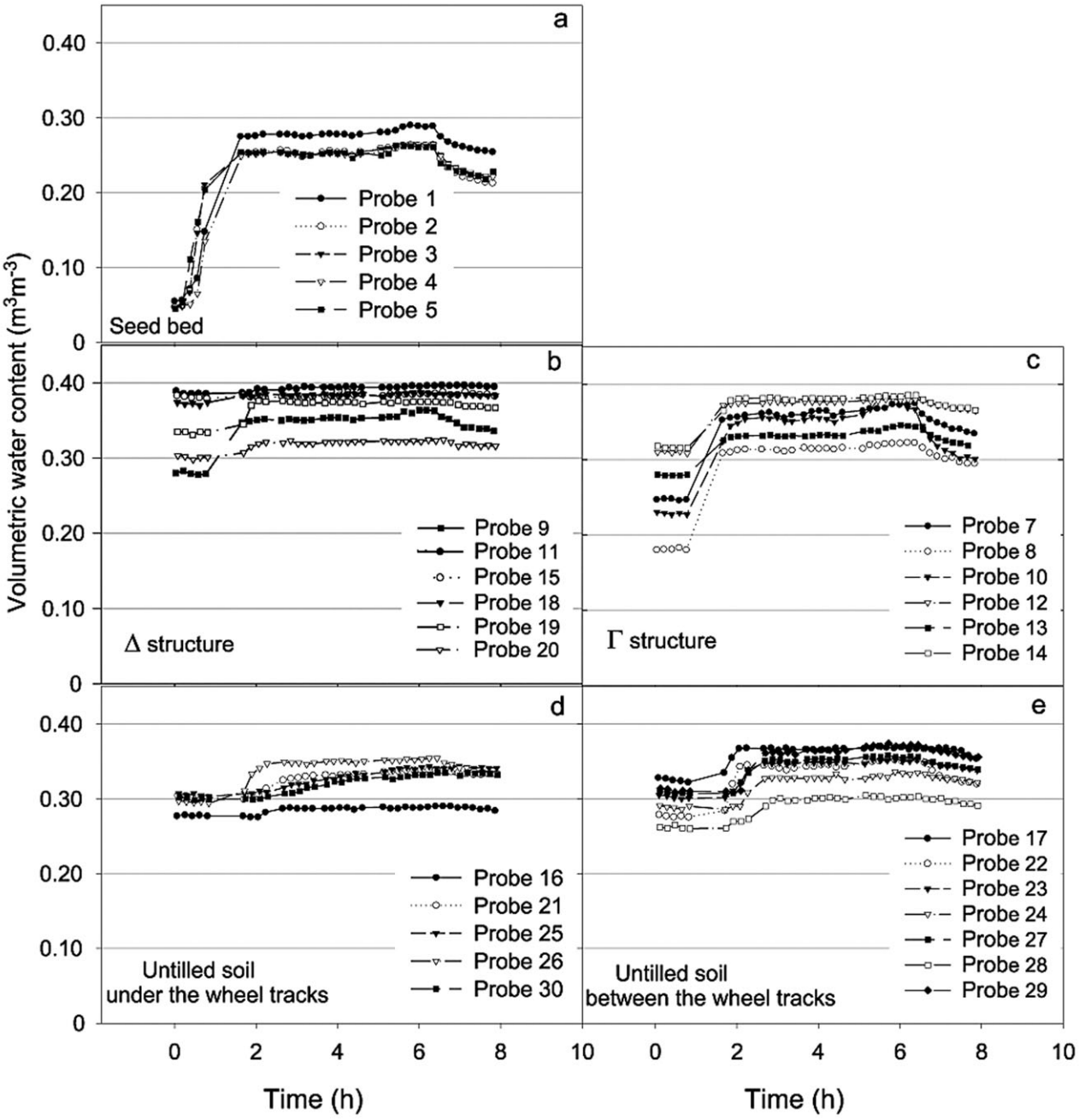

Fig. 4. Time domain reflectometry (TDR) probe responses to infiltration.

sharp increases in pressure head as the water front reached the ceramic cups. The first tensiometers to record the arrival of the infiltration front (Probes 1, 7, 13, and 25) were located at the shallowest depth (3 cm) in the seed bed. The other tensiometers responded later, but not in a consistent manner in terms of their depths. Except for 13, all tensiometers reacted later than the TDR probes. One possible explanation for this is the discrepancy between the sampling volumes of the relatively small tensiometers (0.6 cm diam., 2 cm long) and the TDR probes (8 cm wide, 20 cm long). Because of their larger sampling volume (Ferré et al., 1998, 2002; Caron et al., 1999), the TDR probes may have detected the infiltration front earlier that the tensiometers. This lag in the response of tensiometers relative to the TDR probes may have been due in part also to the fact that tensiometers generally have a response time of several minutes when outfitted with manometers (Klute and Gardner, 1962; Vachaud, 1969).

Only one tensiometer (15) gave useful results for the Γ zones of the plow layer (Fig. 5c), indicating that the moisture front passed this tensiometer after 1.8 h. All tensiometers in the Δ zones and clods (Fig. 5b) showed a relatively gradual increase in the pressure head, except tensiometer 4. Although placed at the base of a wheel track (Fig. 2a), this tensiometer was located in a slightly less compacted zone below the 16-cm wide spacing between the main and dual tires of the tractor. Tensiome-

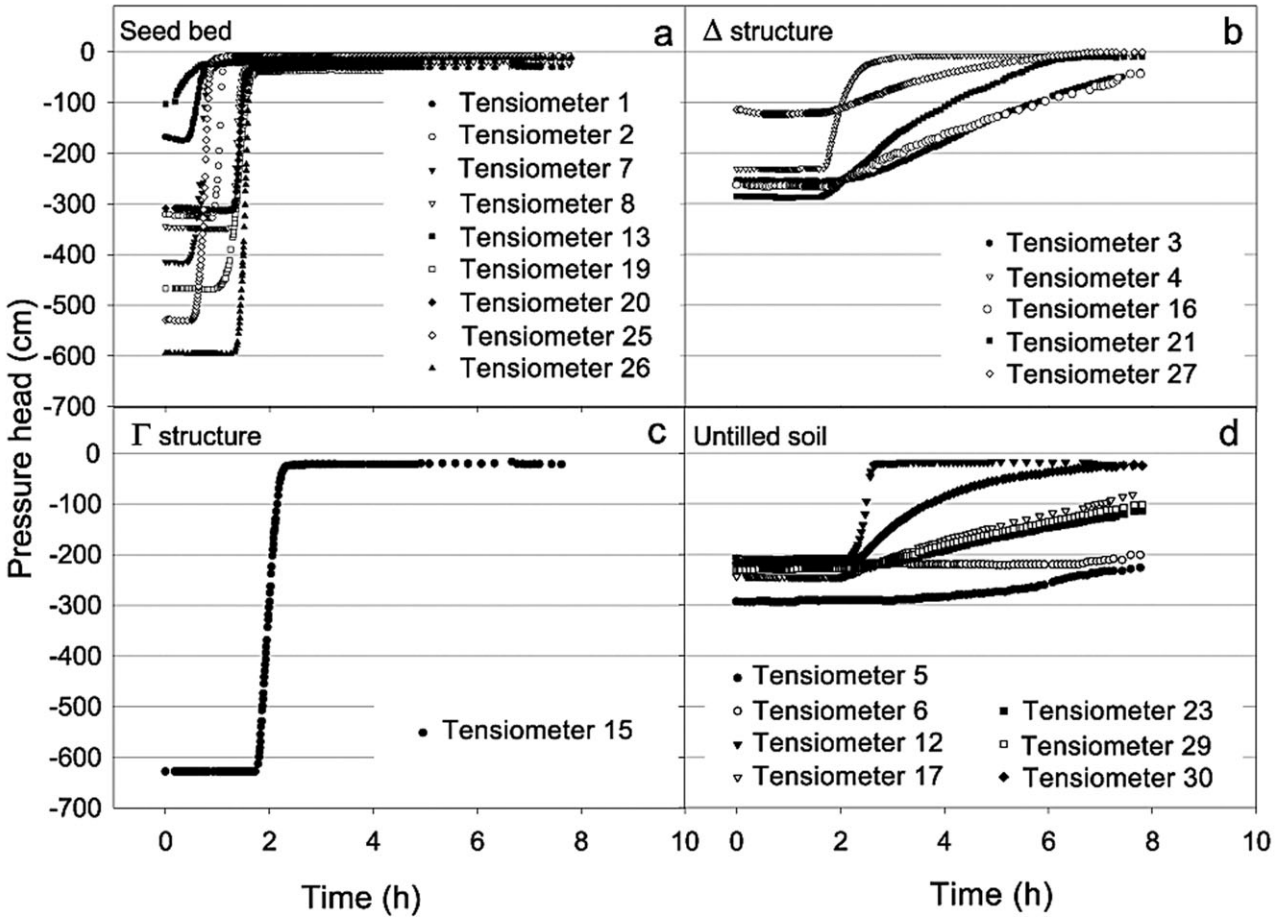

Fig. 5. Tensiometer responses to infiltration.

ter 4 started to react at 1.7 h, approximately the same time as tensiometer 15 at a depth of 22 cm in a Γ zone with a considerable amount of organic matter residues (just below a Δ clod). The pressure head recorded by tensiometer 27, located at the edge of a Δ clod, responded early at 1.2 h, but changed only very slowly in time because of slow movement of water from the neighboring Γ zone toward the Δ clod. Tensiometers 16 and 21 responded similar to tensiometer 27, whereas tensiometer 3, located in the low-permeability compacted Δ zone below the right main tire track, responded the slowest (after 2 h).

Initial pressure heads in the deeper untilled soil layer (Fig. 5d) measured with seven tensiometers (three other tensiometers in this zone did not work satisfactorily) varied little, ranging between −200 and −300 cm. Only tensiometer 12 (Fig. 2a) showed a sharp infiltration front at 2.2 h. This is consistent with TDR Probe 26, which recorded the infiltration front after 1.9 h (Fig. 4d). By contrast, tensiometers 17, 23, and 29, located at depths between 34 and 39 cm between the wheel tracks, recorded water arrival between 2.1 and 2.9 h and gave very similar pressure head values. Tensiometers 5 and 6 below the right wheel track (Fig. 2b) barely responded to water addition. Tensiometer 5 started to respond after 3 h, while Tensiometer 6 responded only minimally after 7 h.

Redistribution

Water redistribution started at 6.3 h (i.e., immediately after the end of the rainfall simulation). Water contents during redistribution are often best plotted as a function of the log of time (t) (Fig. 6). Such graphs are typically used for field measurements of the hydraulic conductivity using the internal drainage method (Libardi et al., 1980; Chong et al., 1981), when θ is approximately a linear function of log(t). The end of the infiltration process is reflected by the quick nonlinear drops in θ at the beginning of the plots for most probes, except for those that reacted only minimally to infiltration (Probes 11, 15, and 18 in Fig. 4b and 6b; Probe 16 in Fig. 4d and 6d). After 7.8 h, θ decreased linearly with log(t) for all probes, except for those in the seedbed where the rate of decrease of θ was not steady but increased with log(t). This was likely due to some evaporation during the relatively warm summer of 2001. While the soil surface was covered with plastic, only a few large stones kept the plastic in place. The plastic likely was also somewhat permeable to water vapor. In all, the behavior of the TDR probes during redistribution was consistent with that during infiltration. At the end of the experiment, 42 d after the infiltration, θ was slightly higher than the initial values as measured before the infiltration started.

The tensiometers generally responded very similarly

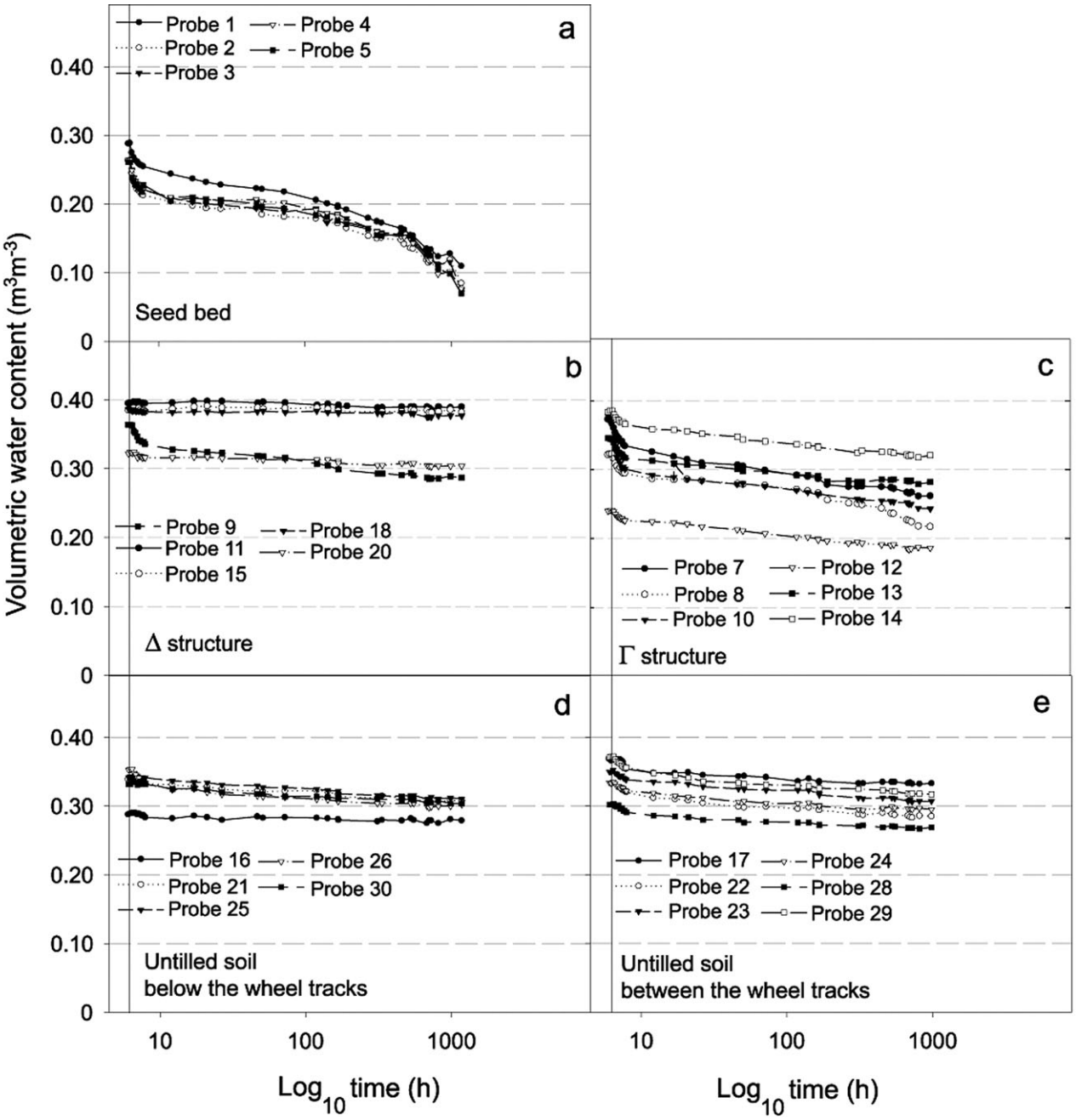

Fig. 6. Water redistribution within the soil profile as recorded with time domain reflectometry (TDR) probes. Vertical bars mark end of infiltration.

as the TDR probes (Fig. 7). For example, the pressure head in the seed bed also decreased with log(t) (Fig. 7a), and at increasing rates near the end of the experiment, again most probably because of some evaporation. The pressure heads may have been more variable also toward the end of the experiment because of temperature effects on the readings during the summer (Haise and Kelley, 1950). Several tensiometers in the compacted soil below the wheel tracks (e.g., tensiometer 3, Fig. 7b) and in the soil undisturbed by tillage (tensiometers 17, 23, 29, Fig. 7d) still recorded increasing pressure heads with time after irrigation ceased (i.e., after 6 h 20 min). This indicates that water was still percolating into these depths of the profile after irrigation had ceased. Shortly afterward, however, the pressure heads in these parts of the profile started to decrease at rates that were quite similar to other locations with the same soil structure (i.e., seed bed, Δ, Γ, or untilled soil).

Solute Concentrations after Infiltration

The soil was sampled for Br^- concentrations 12 h after rainfall simulation. Each square in Fig. 8a represents a sampling location. A kriged contour plot was constructed using the Surfer software (Golden Software, Inc., Golden, CO) for ease of visualization (Fig. 8b). The maps show considerable heterogeneity in the Br^- concentration of both the plow layer and the undis-

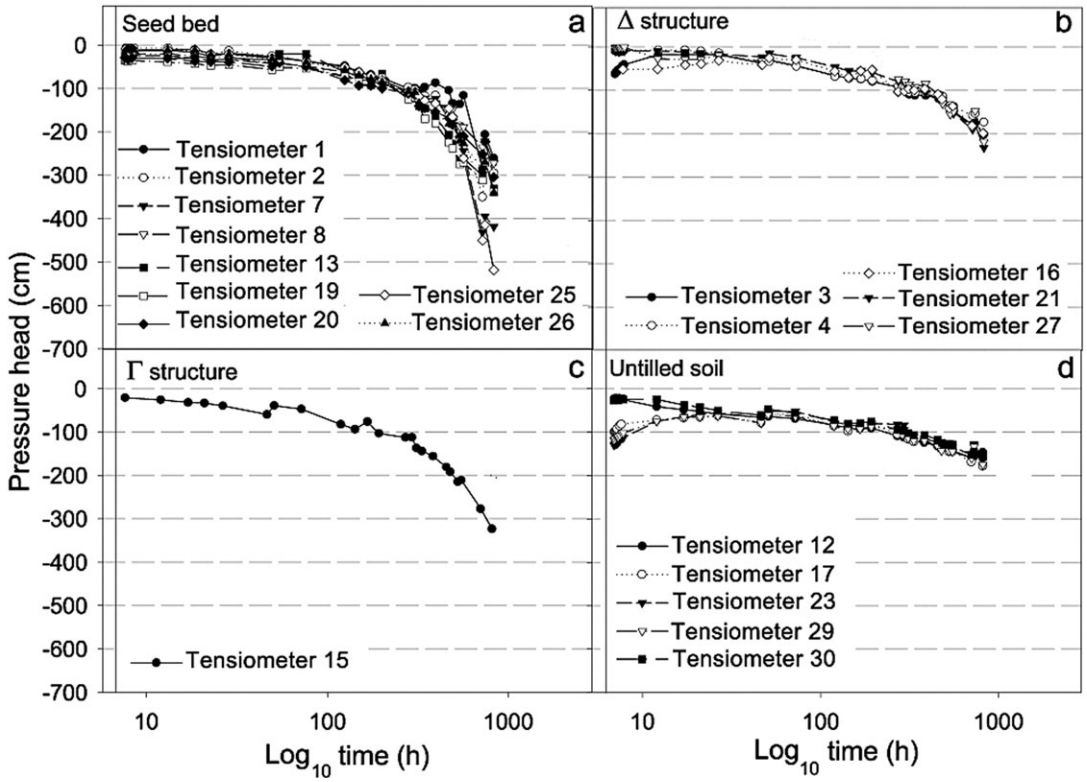

Fig. 7. Water redistribution within the soil profile as recorded with tensiometers. Vertical bars mark end of infiltration.

turbed layer between the wheel tracks. Also, concentrations in the undisturbed deeper layer between the wheel tracks were relatively high next to the wheel tracks. This reflects preferential flow of water and Br^- in the plow layer along the edge of the compacted Δ zones below the wheel tracks. Some Br^- actually reached the bottom of the sampled domain (64 cm), although only 52 mm of Br^- solution had been applied. These results are consistent with the TDR and tensiometer data (Fig. 4 and 5), especially TDR 26 and tensiometer 12 which reacted quickly after irrigation began.

The Δ clods within the plow layer between the wheel tracks had the same effect as the wheel tracks on the infiltration pattern. In Fig. 8, this region of the soil profile is enlarged and compared with the structural map of the soil where the Δ blocks are delineated by white lines. One can see that the advance of the Br^- front was slowed by the Δ clods. Br^- concentrations were lower in these clods (e.g., the clod at x = 120 cm in Fig. 8, where x is the abscissa corresponding to the lateral position within the soil) as well as below these clods (e.g., clods between x = 142 and 154 cm). These results show that the infiltration front moved around these clods. The difference in hydraulic conductivity between the Δ clods and the surrounding Γ soil forces the flow streamlines to diverge around the Δ clods, while impeding flow into the clods themselves as well as the underlying soil, much like an umbrella protects a person from rainfall. This "umbrella effect" of the low-permeability clods is most clearly visible for the Δ clod at x = 120 cm in Fig. 8. This same effect, but at a larger scale, also explains the preferential flow of Br^- around the wheel tracks. Although the average mass balance for the entire plot was 72%, a minimum of only 45% was recovered for a vertical profile through the wheel track at x = 50 cm, while a maximum of 120% was recovered along a vertical concentration profile close to the wheel track at x = 194 cm. These results indicate significant lateral flow and redistribution of infiltrating water toward more permeable nearby zones between the wheel tracks. Similar variabilities in mass recovery rates were observed by Kamau et al. (1996), and also by Schulin et al. (1987) for a stony soil. Schulin et al. (1987) attributed the erratic recovery rates to lateral advective transport caused by water uptake by roots and/or anisotropy in the hydraulic conductivity. We believe that the stones present in their soil may have contributed to lateral transport by creating umbrella effects similar to those observed in our experiment for the Δ zones and clods. Kulli et al. (2003) showed that compaction under wheel tracks can promote preferential flow into earthworm burrows, provided that water ponding occurs at the soil surface. Our study suggests that this same mechanism can be extended to any compacted (Δ) zone within the soil that impedes water and solute fluxes and redirects water laterally toward more permeable (Γ) zones.

Bromide concentrations were found to be the highest in the seed bed. This is consistent with the step-input top boundary condition used for applying the Br^-, along with subsequent advective dispersive transport. Bromide concentrations were lowest in the compacted Δ soil underneath the wheel tracks, although some heterogeneities in the infiltration patterns occurred here also, particularly within the right wheel track at x = 262 cm

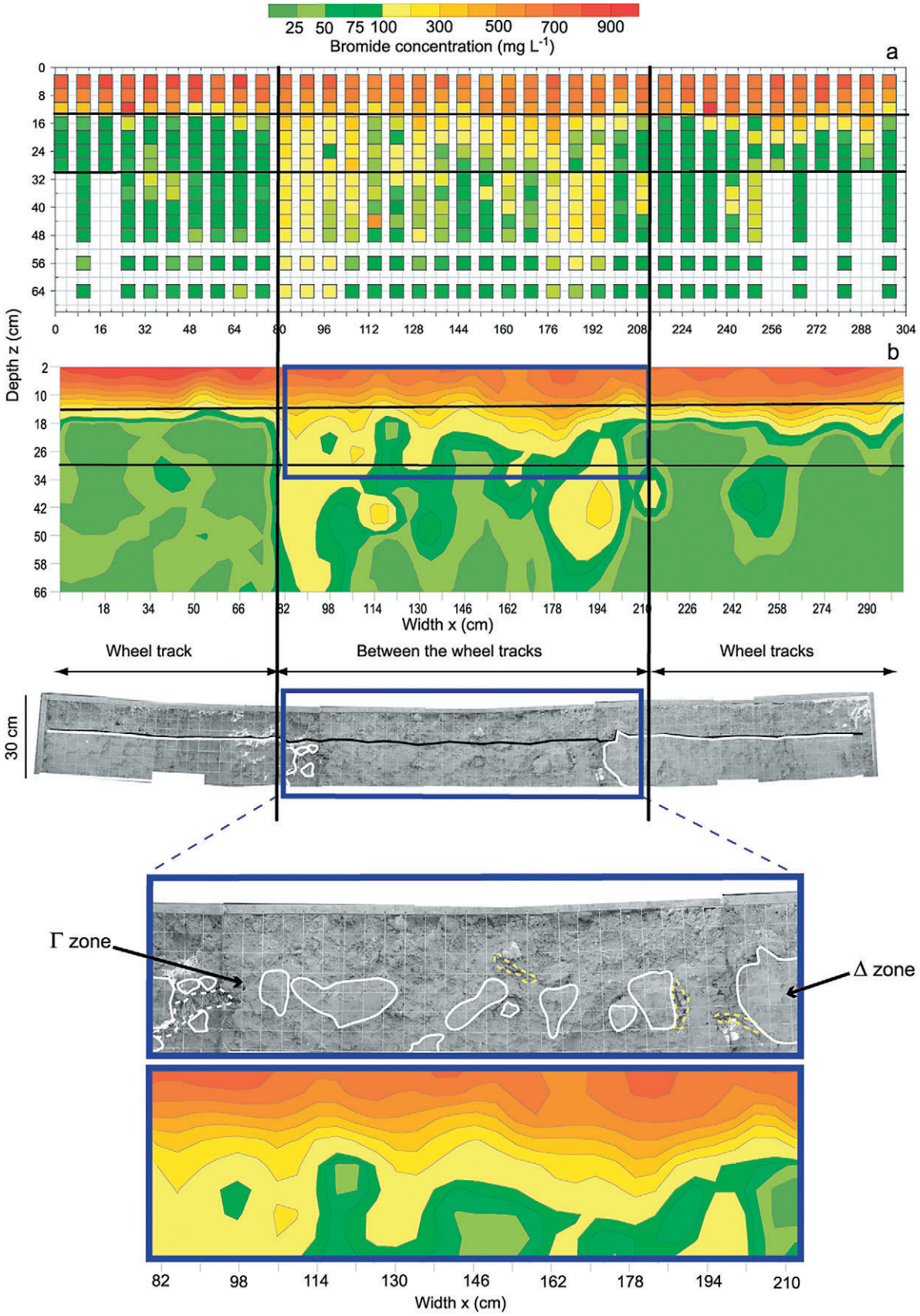

Fig. 8. Observed bromide concentrations within the soil profile in terms of (a) point values, and (b) an interpolated map of concentrations. Enlargements are shown at the bottom of the figure.

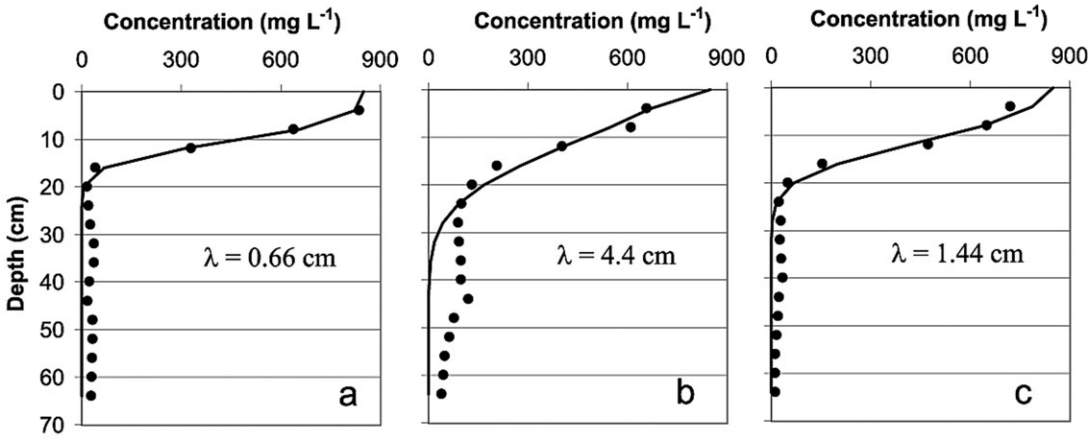

Fig. 9. Average bromide concentration profiles (a) under the left wheel track, (b) between the wheel tracks, and (c) under the right wheel track. Fitted analytical solutions of the one dimensional advection–dispersion equation are shown as solid black lines. Fitted values of soil dispersivity (λ) are also indicated.

(Fig. 8b). This location is between the main and the dual tire (between 252 and 268 cm) where the soil had been slightly less compacted. Again, this is consistent with the relatively fast response of Tensiometer 4 at the base of the wheel track at $x = 260$ cm (Fig. 2a and 5b).

Average concentration profiles below the wheel tracks and between the wheel tracks were obtained by laterally averaging concentrations of vertical Br^- distributions either under the left wheel track, between the wheel tracks, or under the right wheel track (Fig. 9). These profiles were analyzed with an analytical solution of the standard one-dimensional advection–dispersion equation (assuming steady-state water flow) for step inputs using the STANMOD parameter inversion program (Šimůnek et al., 1999). The analytical solution did not account for the effects of preferential flow. The purpose of this analysis was to see if one could obtain an equivalent one-dimensional solute dispersivity by considering a simplified description of the structure of the profile in terms of only compacted soil below the wheel tracks and soil between the wheel tracks. This simplification would allow the use of one-dimensional models to simulate water and solute movement in tilled soils as proposed by Roth et al. (1999). The input concentration was fixed at 850 mg L^{-1}, and the water flux density at 26 mm h^{-1}. The Br^- distribution between the wheel tracks (Fig. 9b) showed a much higher dispersivity (λ = 4.4 cm) than the data below the wheel tracks (0.66 and 1.44 cm). This was expected because of the high heterogeneity of the plow layer between the wheel tracks, which consisted of mixture of compacted and noncompacted clods and soil (Fig. 1). The profile below the right wheel track had a dispersivity twice that of the profile below the left wheel track, thus showing the effect of heterogeneity created by the presence of two types of tires (main and dual) within the same wheel track. Also, notice that the average Br^- concentration profile between the wheel tracks (Fig. 9b) could not be described well with the standard one-dimensional advection–dispersion equation. A significant proportion of the Br^- mass moved to depths beyond 30 cm in this part of the soil. This behavior can be described only using either a one-dimensional dual-porosity transport model or, as shown in the companion study (Coquet et al., 2005), a more elaborate two-dimensional process-based flow/transport model that accounts explicitly for the different heterogeneities in the profile.

SUMMARY AND CONCLUSIONS

Several previous studies have shown that tillage practices can create different types of soil structure within agricultural soils, with each structure having its own hydraulic properties. In this study, a field experiment demonstrated that differences in soil structure created by tillage have a strong impact on the spatial and temporal dynamics of water content and solute concentration. A 4 by 2 m^2 plot was subjected to a step input infiltration of Br^-. After applying 52 mm of the tracer solution, the Br^- front was found to be distributed very heterogeneously in the profile. Little Br^- penetrated the compacted soil below the wheel tracks (moving to a depth of only 17 cm), while the Br^- front moved to a depth of more than 64 cm in areas between the wheel tracks. The heterogeneous leaching pattern was controlled mostly by the presence of compacted soil zones and clods. These compacted zones were not only located below recent wheel tracks, but were also present in the form of large clods between the tracks as a result of the displacement (by plowing) of compacted soil formed under earlier wheel tracks. The compacted clods provided umbrella (or shadow) effects to the infiltrating water, thus causing substantial heterogeneity in the moisture and Br^- fronts.

The abundance, size, and location of compacted clods depend on agricultural practices. Modeling the impact of such clods on water and solute transport may be useful for understanding the potential environmental effects of alternative cropping and tillage systems. In a subsequent paper, a two-dimensional model of water and solute transport is used in attempts to reproduce the field data presented in this paper.

ACKNOWLEDGMENTS

We wish to thank all people involved in this large field experiment, Bernard Renaux from INRA-Orléans, Nathalie Bernet-Lempereur and Valérie Pot from INRA EGC-Grignon, Jacques Troizier and all of the staff of the Experimental Unit of INRA-Grignon. This work was supported by the Research and Education Department of the French Ministry of Agriculture, Alimentation, Fisheries and Rural Affairs. Support from OECD (a fellowship under the OECD Co-operative Research Program: Biological Resource Management for Sustainable Agriculture Systems) and INRA for J. Šimůnek's summer stay at the UMR INRA/INAPG EGC-Grignon is greatly acknowledged.

REFERENCES

Ankeny, M.D., T.C. Kaspar, and R. Horton. 1990. Characterization of tillage and traffic effects on unconfined infiltration measurements. Soil Sci. Soc. Am. J. 54:837–840.

Association Française de Normalisation. 1983. Soil quality. Particle size determination by sedimentation. Pipette method. AFNOR Standard X 31–107. (In French.) AFNOR, Paris.

Association Française de Normalisation. 1995a. Soil quality. Determination of organic and total carbon after dry combustion (elementary analysis). AFNOR Standard NF ISO 10694. (In French.) AFNOR, Paris.

Association Française de Normalisation. 1995b. Soil quality. Determination of carbonate content. Volumetric method. AFNOR Standard NF ISO 10693. (In French.) AFNOR, Paris.

Butters, G.L., W.A. Jury, and F. Ernst. 1989. Field scale transport of bromide in an unsaturated soil. 1. Experimental methodology and results. Water Resour. Res. 25:1575–1581.

Caron, J., S. Ben Jemia, J. Gallichand, and L. Trépanier. 1999. Field bromide transport under transient-state: Monitoring with time domain reflectrometry and porous cup. Soil Sci. Soc. Am. J. 63: 1544–1553.

Chong, S.K., R.E. Green, and L.R. Ahuja. 1981. Simple in situ determination of hydraulic conductivity by power function descriptions of drainage. Water Resour. Res. 17:1109–1114.

Coquet, Y., J. Šimůnek, C. Coutadeur, M. Th. van Genuchten, V. Pot, and J. Roger-Estrade. 2005. Water and solute transport in a cultivated silt loam soil: II. Numerical analysis. Available at www.vadosezonejournal.org Vadose Zone J. 4:587–601 (this issue).

Coutadeur, C., Y. Coquet, and J. Roger-Estrade. 2002. Variation of hydraulic conductivity in a tilled soil. Eur. J. Soil Sci. 53:619–628.

Curmi, P. 1987. Intrinsic physical behavior of clods with different macroporosities. (In French.) p. 53–58. *In* G. Monnier and M.J. Goss (ed.) Soil compaction and regeneration. Proc. of the Workshop on Soil Compaction: Consequences and Structural Regeneration Processes, Avignon, France. 17–18 Sept. 1985. A.A Balkema, Rotterdam, The Netherlands.

Desbourdes-Coutadeur, C. 2002. Study of water transport in a plowed soil. Bidimensional modeling of infiltration and redistribution in soil with an heterogeneous structure. (In French, with English abstract.) Thèse de doctorat de l'Institut National Agronomique Paris-Grignon, INA-PG, Paris.

Deurer, M., W.H.M. Duijnisveld, J. Böttcher, and G. Klump. 2001. Heterogeneous solute flow in a sandy soil under a pine forest: Evaluation of a modeling concept. J. Plant Nutr. Soil Sci. 164: 601–610.

Ellsworth, T.R., and W.A. Jury. 1991. A three-dimensional field study of solute transport through unsaturated, layered, porous media. 2. Characterization of vertical dispersion. Water Resour. Res. 27: 967–981.

Ferré, P.A., J.H. Knight, D.L. Rudolph, and R.G. Kachanoski. 1998. The sample areas of conventional and alternative time domain reflectometry probes. Water Resour. Res. 34:2971–2979.

Ferré, T.P.A., H.K. Nissen, and J. Šimůnek. 2002. The effect of the spatial sensitivity of TDR on inferring soil hydraulic properties from water content measurements made during the advance of a wetting front. Vadose Zone J. 1:281–288.

Flury, M., H. Flühler, W.A. Jury, and J. Leuenberger. 1994. Susceptibility of soils to preferential flow of water: A field study. Water Resour. Res. 30:1945–1954.

Flury, M., J. Leuenberger, B. Studer, and H. Flühler. 1995. Transport of anions and herbicides in a loamy and a sandy field soil. Water Resour. Res. 31:823–835.

Gysi, M., A. Ott, and H. Flühler. 1999. Influence of single passes with high wheel load on a structured, unploughed sandy loam soil. Soil Tillage Res. 52:141–151.

Haise, H.R., and O.J. Kelley. 1950. Causes of diurnal fluctuations of tensiometers. Soil Sci. 70:301–313.

Hammel, K., J. Gross, G. Wessolek, and K. Roth. 1999. Two-dimensional simulation of bromide transport in a heterogeneous field soil with transient unsaturated flow. Eur. J. Soil Sci. 50:633–647.

Kamau, P.A., T.R. Ellsworth, C.W. Boast, and F.W. Simmons. 1996. Tillage and cropping effects on preferential flow and solute transport. Soil Sci. 161:549–561.

Klute, A., and W.R. Gardner. 1962. Tensiometer response time. Soil Sci. 93:204–207.

Kulli, B., M. Gysi, and H. Flühler. 2003. Visualizing soil compaction based on flow pattern analysis. Soil Tillage Res. 70:29–40.

Libardi, P.L., K. Reichardt, D.R. Nielsen, and J.W. Biggar. 1980. Simple field methods for estimating soil hydraulic conductivity. Soil Sci. Soc. Am. J. 44:3–7.

Manichon, H. 1982. Influence of cropping systems on the soil tillage profile: Development of a diagnostic method based on morphological observation. (In French.) Thèse de doctorat de l'Institut National Agronomique Paris-Grignon, INA-PG, Paris.

Mayer, S., T.R. Ellsworth, D.L. Corwin, and K. Loague. 1999. Identifying effective parameters for solute transport models in heterogeneous environments. p. 119–133. *In* D.L. Corwin et al. (ed.) Assessment of non-point source pollution in the vadose zone. Geophysical Monogr. 108. Am. Geophysical Union, Washington, DC.

Meek, B.D., E.A. Rechel, L.M. Carter, and W.R. DeTar. 1989. Changes in filtration under alfalfa as influenced by time and wheel traffic. Soil Sci. Soc. Am. J. 53:238–241.

Mohanty, B.P., M.D. Ankeny, R. Horton, and R.S. Kanwar. 1994. Spatial analysis of hydraulic conductivity measured using disc infiltrometers. Water Resour. Res. 30:2489–2498.

Petersen, C.T., S. Hansen, and H.E. Jensen. 1999. Depth distribution of preferential flow patterns in a sandy loam soil as affected by tillage. Hydrol. Earth Syst. Sci. 4:769–776.

Petersen, C.T., H.E. Jensen, S. Hansen, and C. Bender Koch. 2001. Susceptibility of a sandy loam soil to preferential flow as affected by tillage. Soil Tillage Res. 58:81–89.

Richard, G., H. Boizard, J. Roger-Estrade, J. Boiffin, and J. Guérif. 1999. Field study of soil compaction due to traffic in northern France: Pore space and morphological analysis of the compacted zones. Soil Tillage Res. 51:151–160.

Roger-Estrade, J., G. Richard, H. Boizard, J. Boiffin, J. Caneill, and H. Manichon. 2000. Modelling structural changes in tilled topsoil over time as a function of cropping systems. Eur. J. Soil Sci. 51: 455–474.

Roth, C.H., K.L. Bristow, J. Brunotte, M. Facklam-Moniak, and G. Wessolek. 1999. Impact of tillage and field traffic induced variability of hydraulic properties on unsaturated conductivity and water balance calculations. p. 489–496. *In* M.Th. Van Genuchten et al. (ed.) Characterization and measurement of the hydraulic properties of unsaturated porous media. Part 1. Univ. of California, Riverside.

Roth, K., W.A. Jury, H. Flühler, and W. Attinger. 1991. Transport of chloride through an unsaturated field soil. Water Resour. Res. 27:2533–2541.

Schulin, R., M.Th. van Genuchten, H. Flühler, and P. Ferlin. 1987. An experimental study of solute transport in a stony field soil. Water Resour. Res. 23:1785–1794.

Sillon, J.F. 1999. Experimental and modeling study of the effects of the structure of the plowed layer on the moisture regime of a bare soil during desiccation: Application to the prevision of the available days for cropping operations. (In French, with English abstract.) Thèse de Doctorat de l'Institut National Agronomique Paris-Grignon, INRA-Unité d'Agronomie, Laon.

Šimůnek, J., M.Th. van Genuchten, M. Šejna, N. Toride, and F.J. Leij. 1999. The STANMOD Computer Software for Evaluating Solute Transport in Porous Media Using Analytical Solutions of the Con-

vection-Dispersion Equation. Version 2.0. U.S. Salinity Lab., ARS, USDA, Riverside, CA.
Vachaud, G. 1969. Measurement of capillary pressures in unsaturated soils. (In French) Bull. du B.R.G.M. (deuxième série). Sect. III 4:15–20.
Vanderborght, J., C. Gonzalez, M. Vanclooster, D. Mallants, and J. Feyen. 1997. Effects of soil type and water flux on solute transport. Soil Sci. Soc. Am. J. 61:372–389.
Vanderborght, J., M. Vanclooster, A. Timmerman, P. Seuntjens, D. Mallants, D.J. Kim, D. Jacques, L. Hubrechts, C. Gonzalez, J. Feyen, J. Diels, and J. Deckers. 2001. Overview of inert tracer experiments in key Belgian soil types: Relation between transport and soil morphological and hydraulic properties. Water Resour. Res. 37:2873–2888.
van Wesenbeck, I., and G. Kachanoski. 1994. Effect of variable horizon thickness on solute transport. Soil Sci. Soc. Am. J. 58:1307–1316.
Young, I.M., J.W. Crawford, and C. Rappoldt. 2001. New methods and models for characterising structural heterogeneity of soil. Soil Tillage Res. 61:33–45.